

Crystal Structure, Hydrogen Bonding, and ^{81}Br NQR of Low-Temperature Phase of 4-Aminopyridinium Tetrabromoantimonate(Ⅲ)

Masao Hashimoto,* Hiromitsu Terao,† Hartmut Fuess,†† Ingrid Svoboda,†† and Helmut Ehrenberg††

Department of Chemistry, Faculty of Science, Kobe University, Nadaku, Kobe 657-8501

†Department of Chemistry, Faculty of Integrated Arts and Sciences, Tokushima University, Tokushima 770-8502

††Institute for Materials Science, Darmstadt University of Technology, Petersenstrasse 23, Darmstadt D-64287, Germany

(Received October 8, 2002)

The crystal structure of the low-temperature phase (LTP) of the title compound was determined at 220 K (monoclinic, $P2_1/c$). The 4-aminopyridinium cations (4-$NH_2C_5H_4NH^+$) were found to be ordered in LTP, while being severely disordered in the room-temperature phase (monoclinic, $C2/c$). The tetrabromoantimonate anions ($SbBr_4^-$) were incorporated into the infinite polyanion chains of irregular $SbBr_6$ octahedra with two-edges sharing. The *trans*-Br–Sb–Br moiety in the $SbBr_4^-$ anion was approximately symmetric differing from the asymmetric Br–Sb···Br moiety found in LTP of pyridinium tetrabromoantimonate(Ⅲ). The N–H moieties in both of the pyridine ring and the amino (–NH_2) group participate in the formation of N–H···Br hydrogen bonds. It was shown that the ^{81}Br NQR spectrum of LTP is closely related to the anion structure and the hydrogen bonds. The distinctive anion structures, as well as the different types of phase transitions, exhibited by the PyH and 4-APyH salts, seemed to be attributable to the difference in the hydrogen bond scheme between them.

It has been well known that halogenoantimonates(Ⅲ) with organic cations tend to undergo phase transitions, depending on temperature and/or pressure.[1–3] As we reported previously, the title compound, 4-aminopyridinium tetrabromoantimonate(Ⅲ) [4-$NH_2C_5H_4NH$]$SbBr_4$ (4-APyH salt), undergoes a first-order phase transition at 224 K.[4] For a related compound, pyridinium tetrabromoantimonate(Ⅲ) [C_5H_5NH]$SbBr_4$ (PyH salt), Okuda et al. found a phase transition at 251 K, though it is of second-order.[5]

The crystal structure of the room-temperature phase (RTP) of the PyH salt (space group $C2/c$) reported by DeHaven and Jacobson[6] is characterized by the infinite chain of severely distorted $SbBr_6$ octahedra formed through edge-sharing. The asymmetric anion unit ($SbBr_4^-$) has two crystallographically independent Br atoms, i.e., the bridging and terminal ones (Br(b) and Br(t), respectively). The Sb atom is linked to four Br(b)'s and two Br(t)'s in each octahedron. In the $SbBr_4^-$ ion, one can find a linear *trans*-Br(b)–Sb–Br(b) moiety to which two Br(t)'s are attached at approximately right angles. On a *cis*-Br(t)–Sb–Br(t) plane there exists a two-fold axis passing through the Sb atom and bisecting the Br(t)···Br(t) vector.

Recently, Yamada et al.[7] investigated the structure of the low-temperature phase (LTP) of this salt (space group $P\bar{1}$). It was found that the two-fold axis is lost in LTP and that the asymmetric unit contains four crystallographically independent Br atoms, i.e., two bridging ones (Br(b)′ and Br(b)″), and two terminal ones (Br(t)′ and Br(t)″). They have reported a remarkable difference in the bridging Sb–Br bond lengths between RTP and LTP. According to them, this type of deformation is well consistent with the results for ^{81}Br NQR, and is explainable within the framework of the hypervalent bonding of Sb in $SbBr_6^-$ or three-center four-electron (3c–4e) bonding in the linear Br–Sb–Br unit.

An investigation of the crystal structure of RTP of the 4-APyH salt has indicated that the anion structure is quite similar to that found in the PyH salt.[4] Recently, we reported on the temperature dependences of T_1 and T_2 of ^{81}Br and ^{121}Sb NQR for the 4-APyH salt.[8]

We have been interested in the fact that the 4-APyH salt undergoes a first-order phase transition, and that the temperature dependence of ^{81}Br NQR frequency (ν) of the salt is considerably different from that of the PyH salt.[4,5] In the present work, we determined the structure of LTP of the 4-APyH salt to clarify the structural difference between LTP's of the 4-APyH and PyH salts and to obtain information on the difference in the mechanism of phase transitions between the two compounds.

Experimental

The 4-APyH salt was prepared by a method reported elsewhere.[4] Single crystals suitable for X-ray experiments were grown from a dilute HBr solution of the salt.

Intensity data were measured with a Stoe-stadi4 diffractometer at 220 K. Crystal data are listed in Table 1, together with the experimental details. The structure was solved by a direct method (SHELXS-86)[9] and refined by a full-matrix least-squares method with a program (SHELXL-93).[10] The non-hydrogen atoms were refined with anisotropic thermal parameters. The positions of the two hydrogen atoms in the amino group and the one attached to the pyridine-N atom were refined with isotropic thermal parameters. The positions of the other hydrogen atoms were calculated and fixed in the refinement. The weighting scheme was $w = 1/[\sigma^2(F_o^2) + (aP)^2 + bP]$, where $P = (F_o^2 + 2F_c^2)/3$. Crystallographic data have been deposited at the CCDC, 12 Union Road, Cambridge CB2 1EZ, UK and copies can be obtained on request, free from charge, by quoting the publication citation and the deposition number 199843.

Table 1. Crystal Data and Experimental Details

Empirical Formula		$C_5H_7Br_4N_2Sb$
Formula weight		536.52
Temperature/K		220
Diffractometer		Stoe-Stadi4
Radiation		Mo Kα
Wave length/Å		0.71069
Crystal System		monoclinic
Space group		$P2_1/c$
a/Å		11.548(3)
b/Å		14.029(5)
c/Å		7.432(2)
β/°		93.19(2)
Z		4
Volume/Å^3		1202.2(6)
D_{calc}/g cm^{-3}		2.964
Crystal size/mm		0.80 × 0.38 × 0.13
Absorption correction		numeric
$2\theta_{max}$/°		56
μ/mm^{-1}		15.546
$F(000)$		968
Range of h		$-15 \rightarrow 15$
Range of k		$-18 \rightarrow 8$
Range of l		$0 \rightarrow 9$
No. of reflections	total	4878
	unique	2906
	($I > 2\sigma(I)$)	2497
No. of parameters		119
R (int)		0.0306
R ($I > 2\sigma(I)$)		0.0312
$wR(F^2)$ for all data		0.0823
Goodness-of-fit on F^2		1.086
Extinction coefficient		0.00022(13)
Weighting parameters		
a		0.0520
b		0.06
$\delta\rho$/e Å^{-3}		+1.09, −1.45

Results and Discussion

The fractional atomic coordinates for LTP of the 4-APyH salt at 220 K are listed in Table 2. A part of the structure of LTP projected onto the *ab* plane is illustrated in Fig. 1 to explicitly show the $SbBr_6$ octahedra and possible N–H···Br hydrogen bonds. The atom numbering is also given in the figure. The anionic chains in LTP are shown in Fig. 2 (a). The two bridging Br atoms (Br4(b) and Br5(b)) of the $SbBr_4^-$ anion in LTP participate in the formation of an infinite polyanion chain connected by two edges sharing the distorted $SbBr_6$ octahedra, two terminal Br atoms (Br2(t) and Br3(t)) being free from sharing. This structure of an anionic chain is quite similar to that in RTP (Fig. 2 (b)), except for the loss of the two-fold axis passing through the Sb atom.

RTP of the 4-APyH salt gives an ^{81}Br NQR line at ca. 122 MHz assigned to the terminal bromine atom, while the spectrum splits into two lines at ca. 132 and ca. 115 MHz (assigned to Br2(t) and Br3(t)) in LTP.[4] The splitting of the NQR spectrum is consistent with the loss of the two-fold symmetry in LTP. The NQR frequency splitting ($\Delta\nu$) is almost constant with a relatively large value of ca. 17 MHz throughout the observed temperature range, though the bond lengths of Sb–Br2(t) and Sb–Br3(t) are similar:

Table 2. Atomic Coordinates ($\times 10^4$) and Equivalent Isotropic Displacement Parameters (B_{eq}/Å^2) for LTP of 4-Aminopyridinium Tetrabromoantimonate(Ⅲ) at 220 K

Atoms	x	y	z	B_{eq}
Sb1	2609(1)	1667(1)	5214(1)	1.87(1)
Br2*	4066(1)	546(1)	6820(1)	2.43(1)
Br3*	1381(1)	291(1)	3748(1)	2.70(1)
Br4*	3996(1)	1686(1)	2230(1)	2.48(1)
Br5*	1146(1)	1626(1)	8129(1)	2.51(1)
N6	6733(4)	1684(3)	4792(7)	3.57(1)
C7	7221(3)	2523(3)	5102(5)	2.41(1)
C8	6663(4)	3381(4)	4555(7)	3.39(1)
C9	7189(6)	4217(4)	4920(8)	4.53(1)
N10	8238(5)	426(4)	5799(7)	4.82(1)
C11	8812(5)	3470(4)	6325(7)	3.94(1)
C12	8342(3)	2590(3)	5975(6)	2.72(1)

∗ Br2, Br3, Br4, and Br5 are referred to in the text as Br2(t), Br3(t), Br4(b), and Br5(b), respectively, to distinguish terminal and bridging atoms explicitly.

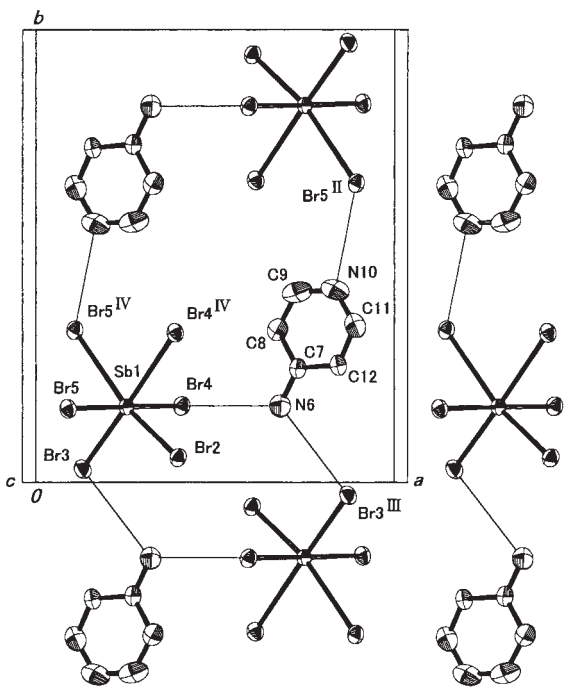

Fig. 1. Arrangement of $SbBr_6$ octahedra and cations in LTP of 4-Aminopyridinium tetrabromoantimonate(Ⅲ) viewed along the *c* axis. Possible N–H···Br hydrogen bonds are indicated by thin solid lines. Anion chains are not shown to indicate the octahedra and the hydrogen bonds clearly. In the text, Br2, Br3, Br4, and Br5 are referred to as Br2(t), Br3(t), Br4(b), and Br5(b), respectively, to distinguish terminal and bridging atoms explicitly.

2.551(1) and 2.599(1) Å, respectively (Table 3). The $\Delta\nu$ value between the terminal Br atoms in LTP of the 4-APyH salt is compared with the corresponding $\Delta\nu$ observed in LTP of the PyH salt, which increases from zero at $T_c = 251$ K to ca. 14 MHz at 77 K.[5] In the latter compound, the lengths of the terminal bonds are 2.569(2) and 2.580(2) Å, respectively.

In the case of the bridging Br atom, however, a remarkable

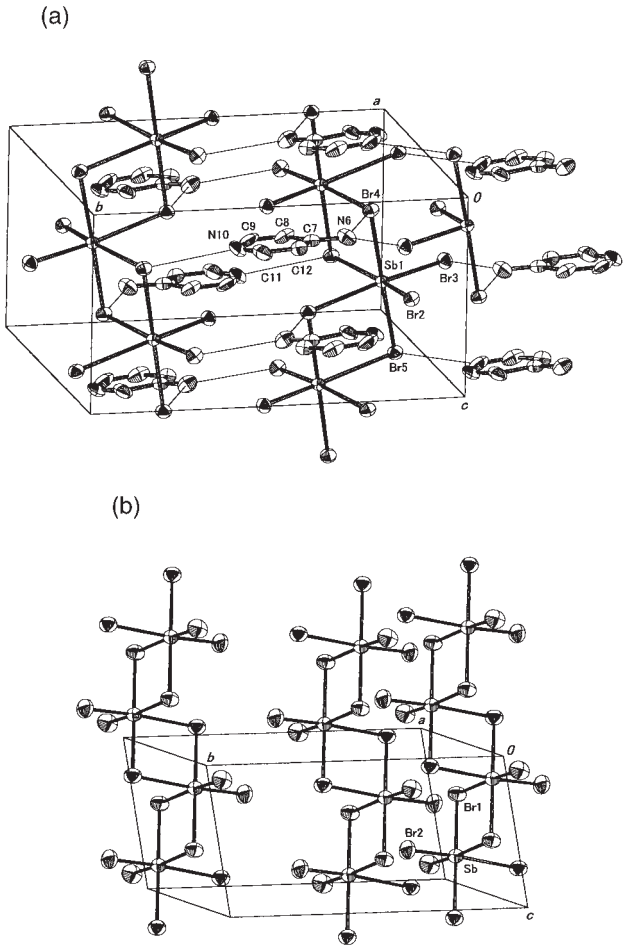

Fig. 2. Comparison of the crystal structures of LTP and RTP of 4-Aminopyridinium tetrabromoantimonate(Ⅲ). (a) LTP; thin solid lines indicate N–H···Br hydrogen bonds. (b) RTP without cations (crystal data for RTP: monoclinic, space group $C2/c$, $a = 13.842(2)$, $b = 13.778(3)$, $c = 7.555(2)$ Å, $\beta = 121.58(1)^\circ$).[4] The unit cell of LTP is approximately related to that of RTP as follows: $a_{RTP} = a_{LTP} + c_{LTP}$, $b_{RTP} = -b_{LTP}$, $c_{RTP} = -c_{LTP}$.

difference in the NQR spectrum can be seen between the two salts. That is, two ^{81}Br NQR frequencies assigned to the bridging Br atoms in LTP of the PyH salt are strongly temperature dependent and the value of $\Delta\nu$ increases steeply from zero at T_c to ca. 50 MHz at 77 K with decreasing temperature,[5] while the corresponding $\Delta\nu$ observed for the 4-APyH salt shows almost a constant value of only ca. 2 MHz throughout LTP.[4] Yamada et al. recognized that the difference in the bond length (ΔL) between Sb–Br(b)′ (2.724 Å) and Sb–Br(b)″ (2.934 Å) in the *trans*-Br(b)′–Sb–Br(b)″ moiety was considerably large. Thus, they suggest that the extremely large $\Delta\nu$ in the PyH salt is explainable by a ΔL value of ca. 0.21 Å, indicating a considerable difference in the bond nature between the two bonds.[7] In the case of the 4-APyH salt, however, the lengths of the Sb–Br4(b) and Sb–Br5(b) bonds in the *trans*-Br4(b)–Sb–Br5(b) moiety are 2.821(1) and 2.807(1) Å, respectively. The small ΔL value of 0.014 Å between the two bonds is consistent with the relatively small $\Delta\nu$ value observed in LTP of the 4-APyH salt, indicating an approximate equivalence in their bond nature.

Table 3. Selected Sb–Br Bond Lengths (Å) and Bond Angles (degrees) Related to the Geometry of the Anion Chain and Short Intermolecular Br···N Contacts (Å) in LTP of 4-Aminopyridinium Tetrabromoantimonate(Ⅲ) at 220 K

Lengths			
Sb1–Br2	2.551(1)	Br4···N6(amine)	3.599(5)
Sb1–Br3	2.599(1)	Br3^{Ⅲ}···N6(amine)	3.651(5)
Sb1–Br4	2.807(1)	Br2^{Ⅲ}···N6(amine)	3.456(5)*
Sb1–Br5	2.821(1)	Br5^{Ⅱ}···N10(pyridine ring)	3.474(5)
Sb1–Br4^{Ⅳ}	3.144(1)		
Sb1–Br5^{Ⅳ2}	3.271(1)		
Bond angles			
Br2–Sb1–Br3	93.92(3)	Br2–Sb1–Br4	89.14(2)
Br2–Sb1–Br5	92.04(2)	Br2–Sb1–Br4^{Ⅳ}	85.70(3)
Br2–Sb1–Br5^{Ⅳ2}	169.44(2)	Br3–Sb1–Br5^{Ⅳ2}	95.16(3)
Br3–Sb1–Br4	89.87(2)	Br3–Sb1–Br5	88.32(2)
Br3–Sb1–Br4^{Ⅳ}	175.99(1)	Br4–Sb1–Br4^{Ⅳ}	94.11(2)
Br4–Sb1–Br5	177.90(1)	Br4–Sb1–Br5^{Ⅳ2}	85.48(2)
Br4^{Ⅳ}–Sb1–Br5^{Ⅳ2}	85.62(3)	Br5–Sb1–Br5^{Ⅳ2}	93.62(2)
Br5–Sb1–Br4^{Ⅳ}	87.72(2)	Sb1–Br4–Sb1^{Ⅳ2}	94.90(2)
Sb1–Br5^{Ⅳ2}–Sb1^{Ⅳ2}	91.90(2)		

Symmetry codes: Ⅱ $(-x+1, y+1/2, -z+3/2)$; Ⅲ $(-x+1, -y, -z+1)$; Ⅳ $(x, -y+1/2, z+1/2)$; Ⅳ2 $(x, -y+1/2, z-1/2)$. *This contact is excluded from an N–H···Br H-bond formation (see, text).

In LTP of the PyH salt, only Br(b)″ of the two Br atoms in the *trans*-Br(b)′–Sb–Br(b)″ moiety participates in the N–H···Br hydrogen bond (H-bond) with a Br(b)″···N(pyridine ring) distance of 3.44(1) Å. In RTP of this salt, however, the two equivalent Br(b) atoms participate in the H-bonds. Yamada et al. pointed out that the elongation of the Sb–Br(b)″ bond and the contraction of the Sb–Br(b)′ bond in LTP were attributable to a combined effect of the asymmetry of the H-bond and the correlation between the two bonds through the 3c–4e bonding.[7] In contrast, both Br atoms of the *trans*-Br4(b)–Sb–Br5(b) moiety in the 4-APyH salt take part in H-bonds, as shown in Fig. 1, i.e., the Br4(b)···N6(amine) and Br5(b)^{Ⅱ}···N10(pyridine ring) contacts given in Table 3 are comparable to Br···N distances corresponding to the H-bonds of this type in related compounds.[11–13] Therefore, it may be presumed that the Sb–Br4(b) and Sb–Br5(b) bonds in LTP of the 4-APyH salt are approximately equivalent owing to the participation of both Br atoms in the H-bonds.

From the examples of the two salts discussed above, we can notice how much the Sb–Br(b) bond lengths are influenced by the H-bonding scheme.

As shown in Table 3, the terminal Br2(t) and Br3(t) atoms also have short contacts of Br2(t)···N6(amine) and Br3(t)···N6(amine), respectively, indicating the possibility of their participation in H-bonding. The former contact, however, does not fit to a geometrical arrangement for the formation of H-bonds including the $-NH_2$ group, while the latter one does. That is, the angle Br3(t)···N6···Br4(b) of ca. 130° is close to the H–N6–H valence angle of the $-NH_2$ group, which allows us to assume simultaneous participation of the two H atoms in H-bonding with Br3(t) and Br4(b). On the contrary, the N6···Br2(t) vector points in such a direction that nearly bisects the H–N6–H angle, as can be seen in Fig. 3 (a). This arrangement of the Br2(t) atom may

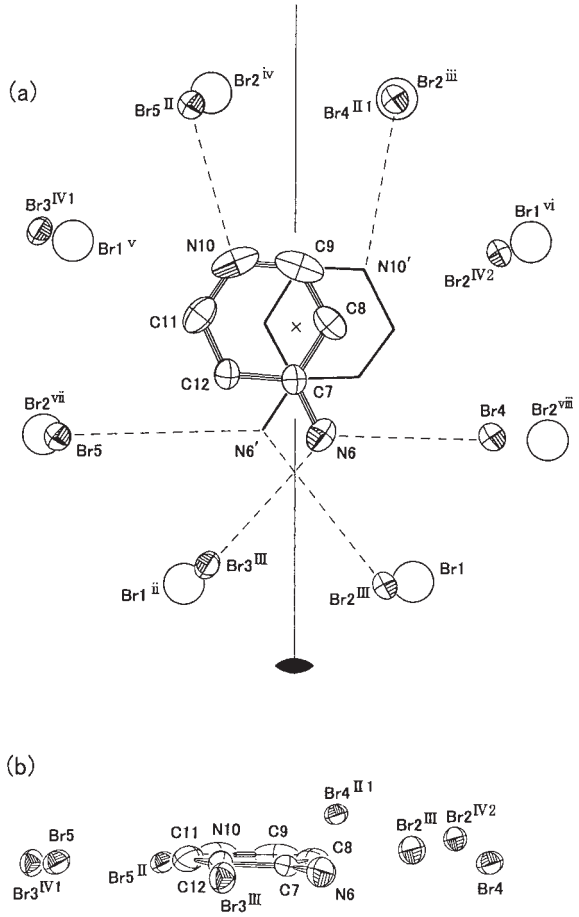

Fig. 3. (a) Top view of the distorted octagons of the Br atoms surrounding the cation in LTP and RTP (large open circles correspond to the Br atoms in RTP). (b) side view of the arrangement of atoms in LTP. The cation given by solid line indicates one of the possible orientations (see text). Broken and bold solid lines indicate the hydrogen bonds and the two-fold axis in RTP, respectively. The symbol × denotes the approximate center of the octagon. Symmetry codes for LTP: II $(-x+1, y+0.5, -z+1.5)$, II1 $(-x+1, y+0.5, z+0.5)$, III $(-x+1, -y, -z+1)$, IV1 $(x+1, -y+0.5, z+0.5)$, IV2 $(x, -y+0.5, z-0.5)$; Symmetry codes for RTP: ii $(-x+1, y, -z+0.5)$, iii $(-x+1, -y+1, -z+1)$, iv $(x, -y+1, z-0.5)$, v $(x+0.5, y+0.5, z)$, vi $(-x+0.5, y+0.5, -z+0.5)$, vii $(-x+1.5, -y+0.5, -z+1)$, viii $(-x+0.5, -y+0.5, z-0.5)$.

indicate a negligible H-bonding interaction with the $-NH_2$ group, if any, since the valence angle of the NH_2 group is considered to be almost maintained. The N···Br contact (3.456 Å) is longer than the sum of van der Waals radii of the Br and N atoms (ca. 3.4 Å) and, therefore, the effect of the contact on the ^{81}Br NQR frequency of Br2(t) is considered to be insignificant.

Since the ^{81}NQR frequency of a Br atom participating in H-bonding tends to decrease,[14–16] one may expect a lower NQR frequency for Br3(t), and hence an increase in the value of $\Delta\nu$ between Br2(t) and Br3(t). Therefore, one may assign the NQR lines at 132 and 115 MHz to Br2(t) and Br3(t) atoms, respectively, and it is reasonable that the $\Delta\nu$ (ca. 17 MHz at 77 K) for the terminal Br atoms in LTP of 4-APyH is slightly larger than that (ca. 14 MHz at 77 K) in PyH salt, whose terminal atoms do not take part in H-bonding.

One can also see that the length of the Sb–Br3(t) bond affected by the H-bond is slightly longer than that of the Sb–Br2(t) bond, being free from it. It should be noted that the effect of the H-bonding on $\Delta\nu$ and ΔL is rather small for the terminal bonds (in the 4-APyH salt) compared to that for the bridging bonds (in the PyH salt).

Despite the structural similarity between RTP of the two salts, the cation in RTP is disordered in the 4-APyH salt, while ordered in the PyH salt. To see the cause of the difference, we examined the environment around the cation in the 4-APyH salt. The anion chains in LTP of the 4-APyH salt are packed so as to leave rigid channels, wherein the cations are piled so as to keep their planes parallel to each other. A short contact of 3.399(6) Å, found between the C7 atom and the adjacent C12 atom (symmetry code: x, $1/2-y$, $z-1/2$), would indicate a weak intermolecular interaction.

A 4-APyH ion in the channel has eight neighboring Br atoms arranged to form a distorted octagon, as shown in Fig. 3 (a). Moreover, the plane of the cation is approximately coplanar to that of the octagon, as can be seen in Fig. 3 (b). Three N–H···Br H-bonds, i.e., one including the N–H on the pyridine ring and the other two including the $-NH_2$ group, seem to work to keep the cation and the octagon coplanar.

The pseudo-octagonal environment in the 4-ApyH salt is substantially maintained in RTP (see Fig. 3 (a)). It is interesting that the PyH ion in both RTP and LTP of the PyH salt also basically has the same surrounding of eight neighboring Br atoms, except for a difference in the H-bonding scheme.

As for the arrangement (in position and orientation) of the 4-APyH ion in the pseudo-octagonal environment in RTP, there are several models that satisfy the crystallographic C_2 symmetry. The first one is that the 4-ApyH ion lies on the two-fold axis. This is similar to the case of the PyH ion in RTP of the PyH salt, where the PyH ion is found to be ordered on a C_2 axis passing through the N atom in the pyridine ring.[7] However, such an arrangement of the 4-APyH ion may be unfavorable in energetics, since the NH_2 group will not be able to take part efficiently in H-bonding in the octagon. The second model is a pair of the ions illustrated in Fig. 3 (a), which are interrelated to each other by a rotation of ca. 60° around an axis passing through the C7 atom and being perpendicular to the ion plane. In this model, there may be two sets of H-bonds; the scheme is depicted with broken lines (N6···Br4(b), N6···Br3^{III}(t) and N10···Br5^{II}(b)) and (N6′···Br2^{III}(t), N6′···Br5(b) and N10′···Br4^{III}(b)). Therefore, this model seems to be favorable in energetics. It should also be noted that the anisotropic elongation of the thermal ellipsoids of the C9, N10, and C11 atoms, compared to that of the C7 atom observed in LTP, seems to be a sign of the occurrence of this model. As a third model, one could assume rotations of the above pair by ca. ±60° around an axis passing through the center of the pair and being perpendicular to the cation plane (depicted by a cross in Fig. 3 (a)). The formation of three N–H···Br bonds per ion appears to be possible in this model, too.

The second and third models lead to disorders due to the distributions of the arrangements of the ion. In addition, one can expect a dynamic disorder caused by the reorientational motions of the 4-APyH ion around its pseudo-hexagonal axis, as evidenced

by a ^{1}H NMR study.[4] A Fourier map corresponding to the 4-APyH ion tells us that the disorder is very complicated; unfortunately, we could not solve the disorder by applying simple models. In reality, the disorder seems to be the result of a complex combination of a superposition of the models mentioned above and the reorientational motions.

The award of a research fellowship to M. H. by the Alexander von Humboldt Foundation is hereby gratefully acknowledged.

References

1 L. Sobczyk, R. Jakubas, and J. Zaleski, *Polish J. Chem.*, **71**, 265 (1997).

2 K. Yamada and T. Okuda, "Chemistry of Hypervalent Compounds," ed by Akiba, Wiley-VCH, New York (1999), Chap. 3.

3 D. K. Seo, N. Guputa, M.-H. Whangbo, M. Hillebrecht, and G. Thiele, *Inorg. Chem.*, **37**, 407 (1998).

4 M. Hashimoto, S. Hashimoto, H. Terao, M. Kuma, H. Niki, and H. Ino, *Z. Naturforsch. A: Phys. Sci.*, **55**, 167 (2000).

5 T. Okuda, K. Yamada, H. Ishihara, M. Hiura, S. Gima, and H. Negita, *J. Chem. Soc., Chem. Commmun.*, **1981**, 979; T. Okuda, Y. Aihara, N. Tanaka, K. Yamada, and S. Ichiba, *J. Chem. Soc., Dalton Trans.*, **1989**, 631; K. Yamada, T. Ohtani, S. Shirakawa, H. Ohki, T. Okuda, T. Kamiyama, and K. Oikawa, *Z. Naturforsch. A: Phys. Sci.*, **51**, 739 (1996).

6 P. W. DeHaven and R. A. Jacobson, *Cryst. Struct. Commun.*, **5**, 31 (1976).

7 K. Yamada, T. Tsuda, C. Holst, T. Okuda, H. Ehrenberg, I. Svoboda, H.-G. Krane, and H. Fuess, *Bull. Chem. Soc. Jpn.*, **74**, 77 (2001).

8 H. Niki, M. Yogi, M. Tamanaha, U. Seto, M. Hashimoto, and H. Terao, *Z. Naturforsch. A: Phys. Sci.*, **57**, 469 (2002).

9 G. M. Sheldrick, "SHELXS-86," Univ. Goettingen, Germany (1990).

10 G. M. Sheldrick, "SHELXL-93, Program for the Refinement of Crystal Structures," Univ. Goettingen, Germany (1993).

11 J. M. Carola, D. D. Freedman, K. L. McLaughlin, P. C. Reim, and W. J. Schmidt, *Cryst. Struct. Comm.*, **5**, 393 (1976).

12 H. Ishihara, Shi-qi Dou, and Al. Weiss, *Bull. Chem. Soc. Jpn.*, **67**, 637 (1994).

13 J. Zaleski, Cz. Pawlaczyk, R. Jakubas, and H. G. Unruh, *J. Phys. Condens. Matter*, **12**, 7509 (2000).

14 T. Sakurai, *Acta Crystallogr.*, **15**, 1164 (1962).

15 L. V. Jones, M. Sabir, and J. A. S. Smith, *J. Chem. Soc., Dalton Trans.*, **1979**, 703.

16 K. Horiuchi, A. Sasane, Y. Mori, T. Asaji, and D. Nakamura, *Bull. Chem. Soc. Jpn.*, **59**, 2639 (1986).